

Myt1l induced direct reprogramming of pericytes into cholinergic neurons

Xing-Guang Liang¹ | Chao Tan² | Cheng-Kun Wang² | Rong-Rong Tao² |
Yu-Jie Huang¹ | Kui-Fen Ma¹ | Kohji Fukunaga³ | Ming-Zhu Huang¹ | Feng Han² 

¹Central Laboratory, School of Medicine, First Affiliated Hospital, Zhejiang University, Hangzhou, China

²Institute of Pharmacology and Toxicology, College of Pharmaceutical Sciences, Zhejiang University, Hangzhou, China

³Department of Pharmacology, Graduate School of Pharmaceutical Sciences, Tohoku University, Sendai, Japan

Correspondence

Ming-Zhu Huang, Central Laboratory, School of Medicine, First Affiliated Hospital, Zhejiang University, Hangzhou, China.

Email: hmzj2002@zju.edu.cn
and

Feng Han, Institute of Pharmacology and Toxicology, College of Pharmaceutical Sciences, Zhejiang University, Hangzhou, China.

Email: changhuahan@zju.edu.cn

Funding information

Project of Science and Technology Department of Zhejiang Province, Grant/Award Number: 2017C33053; National Natural Science Foundation of China, Grant/Award Number: 81503048; Natural Science Foundation of Zhejiang Province, Grant/Award Number: LY15H030007

Summary

Objective: The cholinergic deficit is thought to underlie progressed cognitive decline in Alzheimer Disease. The lineage reprogramming of somatic cells into cholinergic neurons may provide strategies toward cell-based therapy of neurodegenerative diseases.

Methods and results: Here, we found that a combination of neuronal transcription factors, including *Ascl1*, *Myt1l*, *Brn2*, *Tlx3*, and miR124 (5Fs) were capable of directly converting human brain vascular pericytes (HBVPs) into cholinergic neuronal cells. Intriguingly, the inducible effect screening of reprogramming factors showed that a single reprogramming factor, *Myt1l*, induced cells to exhibit similarly positive staining for Tuj1, MAP2, ChAT, and VACHT upon lentivirus infection with the 5Fs after 30 days. HBVP-converted neurons were rarely labeled even after long-term incubation with BrdU staining, suggesting that induced neurons were directly converted from HBVPs rather than passing through a proliferative state. In addition, the overexpression of *Myt1l* induced the elevation of *Ascl1*, *Brn2*, and *Ngn2* levels that contributed to reprogramming.

Conclusions: Our findings provided proof of the principle that cholinergic neurons could be produced from HBVPs by reprogramming factor-mediated fate instruction. *Myt1l* was a critical mediator of induced neuron cell reprogramming. HBVPs represent another excellent alternative cell resource for cell-based therapy to treat neurodegenerative disease.

KEYWORDS

cholinergic neuron, human brain vascular pericytes, neurodegenerative disease, reprogramming, transcription factors

1 | INTRODUCTION

Accumulating evidence has shown that the cholinergic deficit in the brain participates in the pathological process of cognitive dysfunction.^{1,2} The degradation of cholinergic neurons or the dysfunction of cholinergic circuits is associated with deficits in spatial learning and memory in Alzheimer's disease (AD).³⁻⁵ However, no effective treatment had yet been approved for protecting against cholinergic neuron degradation in AD patients.

Emerging studies have suggested that stem cell-based therapies may be a new intervention for neurodegenerative diseases.⁶⁻⁹ The success of stem cell therapy may largely depend on high-efficient supply of desired functional cell types.^{8,10} However, the limited supply of required stem cells, low-efficient conversion technologies, unstable genetic manipulation, and complex ethical controversies are the main challenges in the field.^{11,12} In addition, the risks of stem cell-based interventions include immunological reactions, tumor formation, and unknown long-term health effects.¹³ Notably, the lineage

reprogramming of somatic cells into neurons provided a new approach toward cell-based therapy of neurodegenerative diseases.^{14,15}

The recent discovery of induced pluripotency by means of somatic cell reprogramming in vitro has generated considerable excitement for regenerative medicine.^{16–18} The cell type was not only of vital importance to lineage reprogramming but also of profound relevance with regard to the eventual translational potential toward successful biomedical applications.¹⁹ Niu et al. reported that cortical astroglia can undergo proliferative intermediate progenitors into fully differentiated neurons with higher efficiency by forced expression of SOX2.²⁰ Karow et al. showed that the high-efficiency reprogramming of endogenous pericyte-derived cells of the cerebral cortex into induced neuronal cells by the combined expression of transcription factors *Sox2* and *Ascl1*.²¹ Human brain vascular pericytes (HBVPs) were identified as a component of the neurovascular unit astonishing plasticity, that is, required to form the blood-brain barrier,^{21,22} which represented a new cell type amenable to direct somatic cell conversion and serving as a potential target for reprogramming into induced neuronal cells.¹⁹ The previous study revealed that pericytes-derived neurons appeared to display the hallmarks of GABAergic interneurons²¹; however, whether HBVPs could be converted into functional cholinergic neurons still remains unknown.

In this study, we set out to address whether the optimization of the synergistic action of the reprogramming factors can drive HBVP to be converted into functional cholinergic neurons. Here, we revealed that *Myt1l* was a critical mediator of HBVP-derived cholinergic neuron reprogramming. Our results suggested that HBVPs represent another excellent initial cell resource for reprogramming-based cell therapy to treat neurodegenerative diseases.

2 | MATERIALS AND METHODS

2.1 | Culture of human brain vascular pericytes

Human brain vascular pericytes (ATCC, USA) were grown in Dulbecco's modified Eagle-high glucose medium (Gibco, USA) supplemented with 2% (vol/vol) fetal bovine serum (Gibco, USA), 1% pericyte growth supplement, and 50 U/mL penicillin G and 50 µg/mL streptomycin (Sigma, USA) in a humidified atmosphere containing 5% CO₂ at 37°C.

2.2 | Lentivirus vector construction

The *Ascl1*, *Myt1l*, *Brn2*, *miR124*, *Tlx3* sequences were obtained from the NCBI and miRBase sequence database. The GV166 (*Myt1l*), GV159 (*miR124*), GV286 (*Brn2*), GV287 (*Ascl1*, *Tlx3*) vector (Genechem, China) was linearized using the restriction enzyme EcoRI (New England Biolabs), and the pGC-CMV-GFP vector (Genechem) was linearized using AgeI and EcoRI. To create pGC-LV recombinant vector, a fragment containing reprogramming factors or miR124 sequence was introduced into the indicated vectors as shown in Figure S2. After that, the pGC-LV recombinant vector was transformed into competent cells. After confirmation by PCR and sequencing, the competent cells, together with the lentiviral packaging vectors pHelper1.0 and pHelper2.0 (Genechem), were

concurrently infected into 293T packaging cells using Lipofectamine 2000 (Invitrogen) to create the virus. The virus titer was determined using the whole dilution method.

2.3 | Transduction assays and retroviral transduction

HBVPs were plated in 24-well plates. When the cells reached 25%–35% confluency, the stage with optimal infection efficiency, the HBVPs were infected with 5 µL of *Ascl1*, *Tlx3*-LV (titer, 1×10^9 transducing units (TU)/mL; multiplicity of infection [MOI], 10), 5 µL of *Brn2*, *Myt1l*, or *miR124*-LV (titer, 1×10^8 TU/mL; MOI, 10) or 2.5 µL of the lentivirus vector alone (titer, 1×10^8 TU/mL; MOI, 10). Retroviral transduction of cultures was performed 2–3 hours after plating on glass coverslips using VSV-G (vesicular stomatitis virus glycoprotein)-pseudotyped retroviruses encoding neurogenic fate determinants. The reprogramming factors were expressed under the control of an internal promoter with a cytomegalovirus enhancer together with *gfp*. For controls, cultures were transduced with a virus encoding only *gfp*. Then, 24 hours after transduction, the medium was replaced by a differentiation medium consisting of DMEM with GlutaMAX, penicillin/streptomycin and B27 supplement (Gibco). Fluorescent protein expression in the HBVPs was observed using inverted fluorescence microscopy at 24, 48, 72, and 96 hours post infection to assess the infection efficiency.

2.4 | Immunocytochemistry, BrdU labeling, and confocal fluorescence imaging

Immunofluorescence was performed with pericytes or pericyte-derived induced neurons. The experimental design for BrdU-labeling experiments is shown in Figure 6C. Cells were incubated with 10 µmol/L of BrdU (Sigma-Aldrich, USA) for the indicated periods of time. Briefly, cells were fixed with methanol at –20°C for 15 minutes, followed by permeabilization in 0.1% Tween-20. Cells were then blocked with 10% FBS for 30 minutes at room temperature and were incubated in PBS containing anti-Desmin, anti-α-NG2, anti-ChAT, anti-VACHT, or anti-BrdU antibody overnight at 4°C. Cells were subsequently washed in PBS three times, after which they were incubated in blocking buffer containing Alexa fluor 488-conjugated anti-mouse IgG (Invitrogen), Alexa fluor 594-conjugated anti-rabbit IgG or Alexa fluor 594-conjugated anti-goat IgG. Nuclei were stained with 4',6-Diamidino-2-phenylindole (DAPI). Fluorescence was obtained with a confocal laser scanning microscope (Olympus, FV1000). Digital images were captured using the FV10-ASW 3.0 viewer software (Olympus). Cell counts were performed using a 40× or 60× objective in at least five fields of view randomly selected from each coverslip. The images shown were representative of three independent experiments.

2.5 | Real-time fluorescent quantitative polymerase chain reaction

Total RNA was isolated using Trizol reagent (Gibco) in accordance with the manufacturer's instructions. To synthesize first strand cDNA, 3 µg

total RNA was incubated with 0.5 μg of oligo (dT) (Sangon, China) at 65°C for 15 minutes. Reverse transcription reactions were performed with 200 units of MMuLV reverse transcriptase, 4 μL of 5 mmol/L reaction buffer, and 1 mmol/L deoxynucleoside triphosphate (dNTP) mixture for 1 hour at 42°C. Polymerase chain reactions of 50 μL contained 1 μL of the reverse transcription reaction product, 5 μL of 10 mmol/L PCR buffer, 25 units Taq polymerase, 1 μL of 10 mmol/L dNTP mixture, and 30 pmol of each primer (Sangon). The reaction using SYBR Premix Ex Taq II kit (Takara) was performed on the CFX96 Real-time PCR detection system (Bio-Rad) with the following procedures: preheating at 95°C for 30 seconds, 39 cycles of 95°C for 5 seconds, and 60°C for 30 seconds. The primer sequences were shown in Table S1 in the supporting information. The $\Delta\Delta\text{C}$ (T) method was used to analyze the relative changes in gene expression. *Gapdh* was used as an internal standard. All data were representative of three independent experiments.

3 | RESULTS

3.1 | Generation of neuron-like cells from HBVPs induced by 5Fs

The concentrated lentivirus-containing reprogramming factors vectors were infected into HBVPs. Immunohistochemical staining has confirmed that cultured HBVPs express the desmin and NG2 (Figure S1). The cell phenotype was recorded from day 1 to day 30 after infection, and a gradual change from HBVPs to cells with typical neuron

morphology was observed. As shown in Figure 1, the HBVPs exhibited a polygonal morphology on day 1 after infection (Figure 1 a1-3), and the body of cell became round on day 5 (Figure 1 b1-3). The axon-like structures from the cell body became longer on day 10 (Figure 1 c1-3) compared to day-5 cells. As the reprogramming time was prolonged, the converted cell exhibited a typical neuron phenotype (day 20 and day 30) and contacted others with long axon (Figure 1d,e). These results suggested that the 5 factors (5Fs) could induce the conversion of HBVPs to cells with neural morphology.

3.2 | Tuj1/MAP2-positive characteristics of 5Fs-induced neuron-like cells

To further characterize the properties of the 5Fs-induced neuron-like cells from HBVPs, we performed immunocytochemistry for the neuronal markers. The results in Figure 2 showed that most of the GFP reporter-positive cells expressed the pan-neuronal marker, microtubule-associated protein 2 (MAP2) (>80%), and neuron-specific class III beta-tubulin (Tuj1), which demonstrated that the converted cells exhibited a neuron-specific protein phenotype. In addition, we noted the existence of MAP2/Tuj1-positive but GFP-negative cells (in the round frames of Figure 2), which indicated that these cells may be induced by *Myt1l* that was not marked with the GFP reporter. A few of the GFP-positive cells were found to be negative or only weakly positive for MAP2 (in the orange frames of Figure 2), raising the possibility that they were partially reprogrammed cells. The MAP2/Tuj1 and GFP double-negative cells that were in the square frames

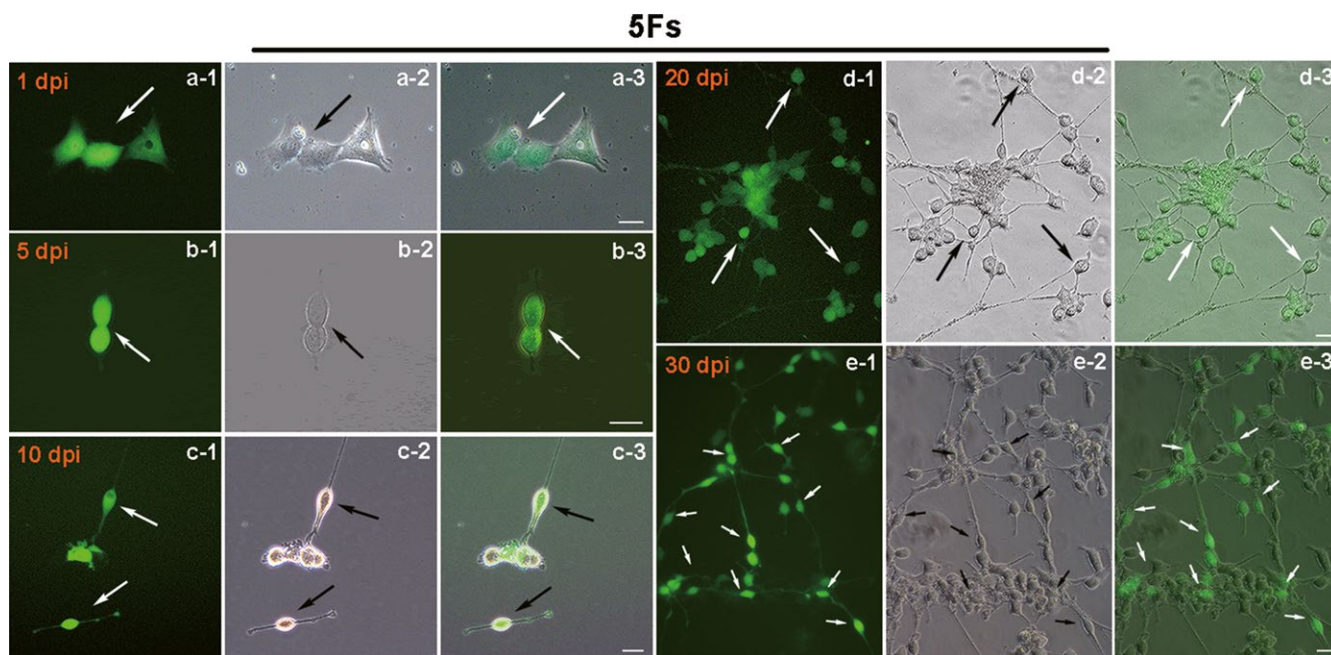


FIGURE 1 Five factors (5Fs) induced the neuronal conversion of human brain vascular pericytes (HBVPs). The time course of reprogramming from day 1 to day 30 after infection with lentivirus-containing reprogramming factors. dpi: day post infection. (a1-a3), 1 dpi. (b1-b3), 5 dpi. (c1-c3), 10 dpi. (d1-d3), 20 dpi. (e1-e3), 30 dpi. (a-e)-1: The fluorescent from GFP indicated the well expression of reprogramming factors. (a-e)-2: bright field of (a-e)-1. (a-e)-3: merge of the picture of -1 and -2. The arrow indicated the typical morphology of transitional HBVPs. All images were representative of three independent experiments ($n = 3$). Scale bar = 25 μm

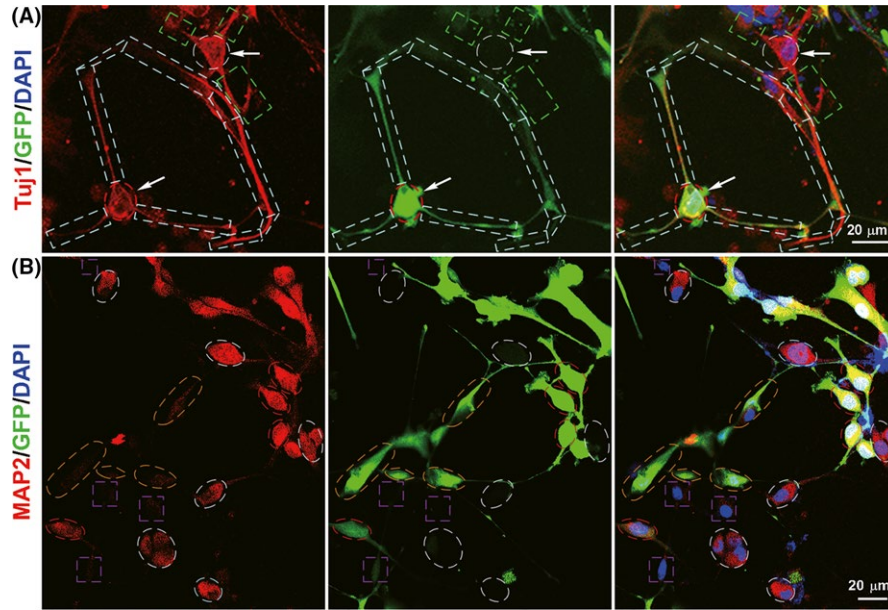


FIGURE 2 5Fs-induced neuron-like cells expressed neuron-specific protein Tuj1 and MAP2 markers. A, Immunocytochemistry showed the expression of Tuj1 (red) in 5Fs-induced neuron-like cells (day 30); GFP fluorescent (green) indicated the expression of reprogramming factors. The arrow indicated the typical morphology of neuron-like cells, and the square frames showed the structure of the nerve axon. B, The 5Fs-induced neurons expressed MAP2 (red). The red, round frames showed MAP2- and GFP double-positive cells that were induced by 5Fs. The white, round frames showed the MAP2-positive but GFP-negative cells that were possibly induced by *Myt1l*. The orange, round frames showed MAP2-negative but GFP-positive cells that were partially reprogrammed, and the square frames indicated the MAP2- and GFP double-negative cells that were not well infected and converted. Nuclei were stained with DAPI (blue). The images shown were representative of three independent experiments ($n = 3$). Scale bar = 20 μm

indicated that these cells were not well infected. From these data, we can see that the 5Fs was able to induce the conversion of HBVPs into Tuj1/MAP2-positive neuron-like cells.

3.3 | *Myt1l* is sufficient to convert HBVPs into cells with a neuron phenotype

To determine which factor was critical for the neuronal conversion of HBVPs, the inducible effect screening of reprogramming factors was conducted. As seen from Figure 3, compared with other factors, *Myt1l*-induced cells exhibited a typical neuronal phenotype in both the early (day 10) and later stage (day 30) of reprogramming (Figure 3A,B). This was an interesting result. Thus, we were keen to know whether *Myt1l* induced cells were similar to those of the 5Fs. As expected, the morphological comparison between *Myt1l*- and 5Fs- induced cells showed that a similar neuron phenotype was observed on day 30 after infection (Figure 3C,D). Taken together, these results suggested that *Myt1l* may be a key factor in the neuronal reprogramming of HBVPs.

3.4 | *Myt1l*/5Fs-induced cholinergic neuron-like cells converted from HBVPs

To determine the subtype of *Myt1l*/5Fs induced neuron-like cells, we further performed immunocytochemistry for cholinergic neuron-specific markers, including choline acetyltransferase (ChAT) and vesicular acetylcholine transporter (VACHT). The former is a key

neuronal enzyme for acetylcholine and is representative of the functional activity of the cholinergic system, and the latter is required in cholinergic neurons for the selective transport of acetylcholine into synaptic vesicles. As seen from the data in Figure 4, the GFP reporter-positive cells exhibited immunoreactivity for ChAT and VACHT (Figure 4B,D), indicating that the 5Fs-induced neuron-like cells were cholinergic neurons. As expected, *Myt1l*-induced neuron-like cells also expressed cholinergic neuron-specific ChAT and VACHT (Figure 4A,C), which indicated that *Myt1l* alone was enough to induce the conversion of HBVPs into cholinergic neurons with specific marker characteristics.

3.5 | *Myt1l* overexpression induced the upregulation of neural transcription factors

As the results above showed that *Myt1l* was sufficient to convert HBVPs into cells with a neuron phenotype, we next explored the effect of *Myt1l* overexpression on reprogramming with related neuronal transcription factors. The expression of other factors after 5 days of infection was confirmed by real-time fluorescent quantitative PCR. As showed in Figure 5, we found a greater increase in *Brn2* and *Ngn2* mRNA expression as well as a moderate enhancement of *Ascl1* mRNA levels in *Myt1l*-induced neuron cells compared to the control group, which suggested that *Myt1l* could up-regulate the expression of other neuronal factors and may act as a critical mediator of neuron reprogramming-based on the cell context of pericytes.

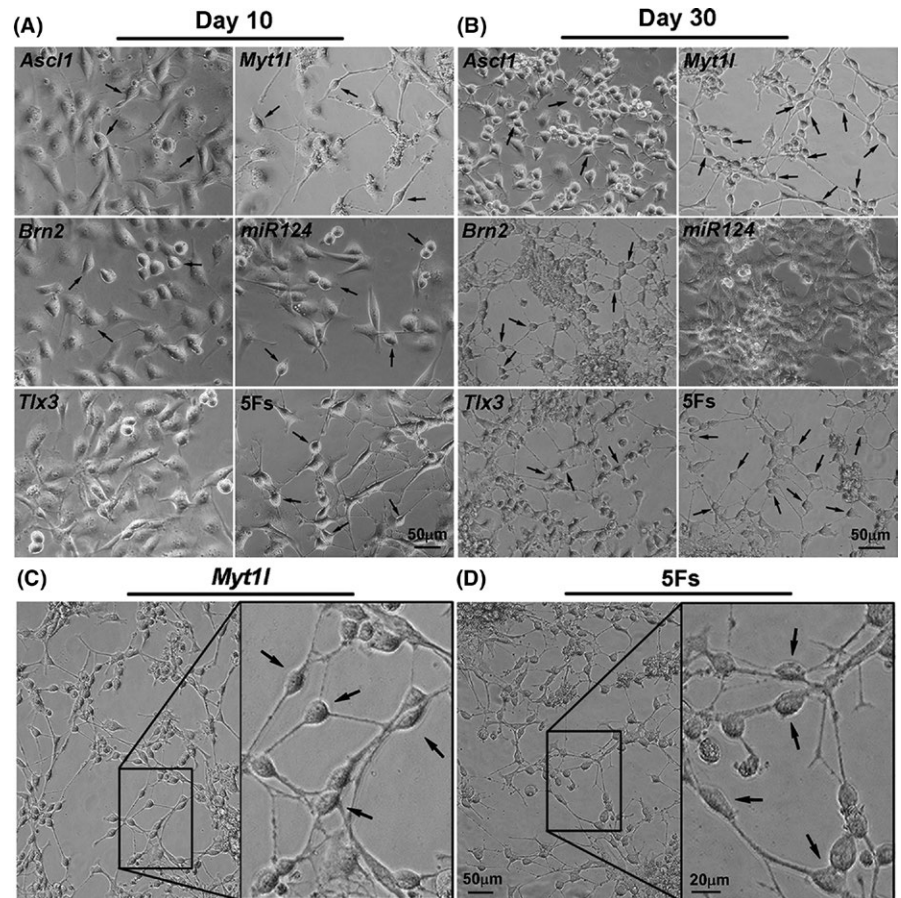


FIGURE 3 *Myt1l*-induced cells exhibited a typical neuron phenotype. A, B, Inducible effect screening of reprogramming factors. Representative images of induced neuron-like cells after induction with a single reprogramming factor, A: 10 dpi, B: 30 dpi. Scale bar = 50 μm. C, *Myt1l* alone on reprogramming into neuron-like cells from HBVPs. D, 5Fs induced neuron-like cells from HBVPs. The right panel is the magnification pane in the left panel. The arrow indicated the typical morphology of transitional HBVPs. Identical results were obtained from three independent experiments (n = 3). Scale bar = 50 μm (left panel of figure C and D), scale bar = 20 μm (right panel of figure C and D)

3.6 | *Myt1l*/5Fs induced neuron-like cells were directly converted from HBVPs

To further explore whether *Myt1l*/5Fs-induced neuron-like cells were directly converted from HBVPs without passing through a proliferative state, cell proliferation was observed during reprogramming and was further examined by 5-bromodeoxyuridine (BrdU)-labeling experiments. From the data in Figure 6A,B, it was apparent that the typical morphology of HBVPs was changed to a neuron-like state from day 10 to day 15. BrdU-labeling experiments showed that HBVPs infected with 5Fs-lentivirus were still labeled with BrdU on day 5 after infection (Figure 6D), while BrdU was rarely labeled in the infected cells but still remained in the nuclei of noninfected cells 10 days after infection (Figure 6E), which indicated that neuronal conversion from HBVPs was accompanied by cell cycle exit.

4 | DISCUSSION

In the current study, we found that a combination of neuronal transcription factors, including *Ascl1*, *Myt1l*, *Brn2*, *Tlx3*, and a microRNA *miR124* (5Fs), were capable of directly converting pericytes into cholinergic neuronal cells. In addition, HBVPs could be induced by a single transcription factor, *Myt1l*, to cells that exhibited a similar neuron phenotype with 5Fs. Reprogramming has been suggested to benefit

from the context of the initial cell. The transcriptome not only facilitated the conversion but also helped to reduce the number of reprogramming factors that are used. Recently, several types of cells were employed in the neural reprogramming in vitro or in situ, such as postnatal fibroblast, astrocytes, and neuroglia cell, indicating that less than three neural transcript factors also successfully elicited the conversion effect.^{19,21-23} For instance, postnatal fibroblasts and embryonic stem cells could be reprogrammed into functional neurons by *Ascl1* alone.²² HBVPs were considered to be a key component of neurovascular unit with multipotent stem cell potential, providing excellent cell context for reprogramming.^{18,22,23} Our present work reported that a single transcription factor, *Myt1l*, is sufficient to direct pericyte reprogramming into cholinergic neuronal cells, also indicating the convenience of HBVPs for neural reprogramming.

Here, *Myt1l*-induced cells exhibited a similar neuron phenotype in both the early and later stages of reprogramming compared with 5Fs, indicating that *Myt1l* may be a key transcription factor of pericyte reprogramming. For its effect on neural fating, *Myt1l* was employed as a neuronal transcription factor in the neuron reprogramming along with other transcription factors such as *Ascl1*, *NeuroD1*, and *Brn2*, which also contributed to determining the neural fate from many different donor cell types.²⁴⁻²⁸ More recently, Wernig et al. revealed that *Myt1l* exerted its proneuronal function by the direct repression of many different somatic lineage programs except the neuronal program, further demonstrating the key role of *Myt1l* in neural reprogramming.²⁹ They

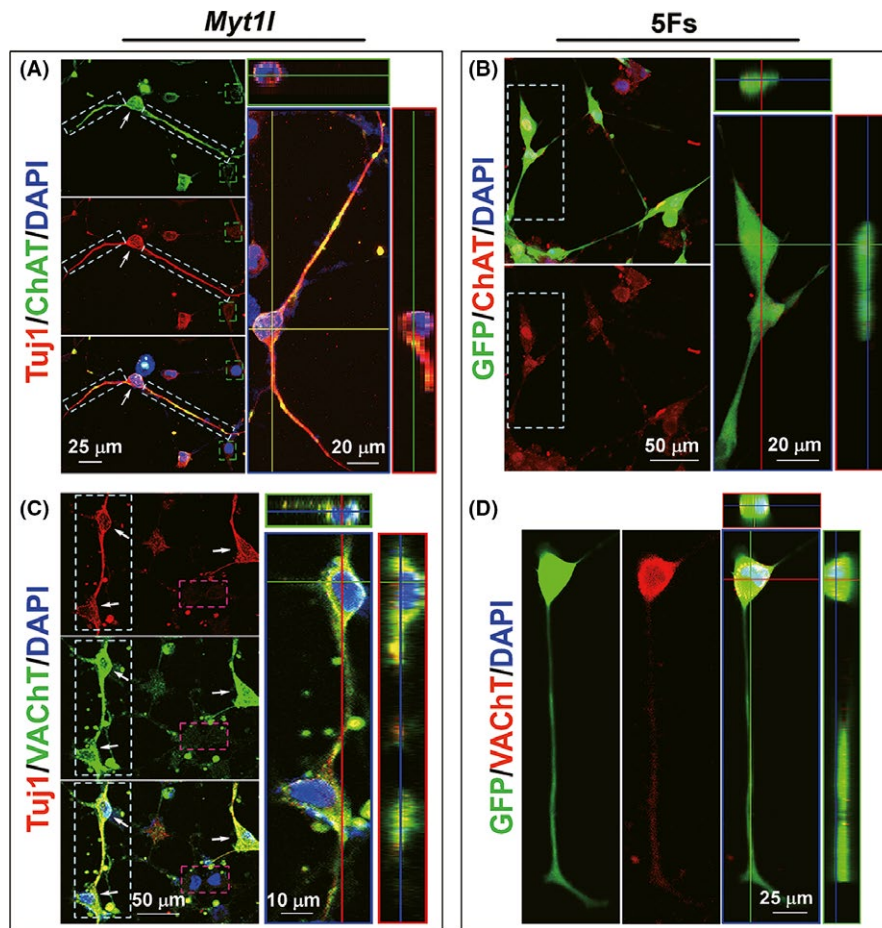


FIGURE 4 *Myt1*-induced neuron-like cells expressed cholinergic neuron-specific proteins ChAT and VACHT. A, Immunocytochemistry showed the expression of Tuj1 (red) and ChAT (green). The arrow indicated the typical morphology of neuron-like cells, the white square frames showed the structure of the nerve axon, and the green square frames indicated the Tuj1 and ChAT double-negative cells that were not well converted. Scale bar = 25 μm (left panel), scale bar = 20 μm (right panel). B, Immunocytochemistry showed the expression of ChAT (red), scale bar = 50 μm (left panel), scale bar = 20 μm (right panel). C, Immunocytochemistry showed the expression of Tuj1 (red) and VACHT (green), and the red square frames indicated the Tuj1 and VACHT double-negative cells that not well converted. Scale bar = 50 μm (left panel), scale bar = 10 μm (right panel). D, Immunocytochemistry showed the expression of VACHT (red), scale bar = 25 μm . Orthogonal projection onto the x-z (upper) and y-z (right) panel as shown to confirm the colocalization of investigated proteins. Nuclei were stained with DAPI (blue). All images were representative of three independent experiments ($n = 3$)

found that *Myt1*-targets such as Notch and Hes1 were significantly downregulated in reprogramming fibroblasts, which indicated that *Myt1* may be a transcriptional repressor that silenced the fibroblast program. In this study, we found that *Myt1* overexpression induced the upregulation of *Ascl1*, *Brn2*, and *Ngn2*, suggesting that *Myt1* could induce the expression of other neuronal transcription factors. According to these data and the finding that brain vascular pericytes exhibited multipotential stem cell activity,³⁰ we can infer that *Myt1* might acted as a critical mediator of neuron reprogramming-based on the cell context of pericytes.

Our findings provided proof of the principle that cholinergic neurons could be produced from HBVPs by transcription factor-mediated fate instruction. As a promising source for a cell-based therapy to treat neurodegenerative diseases, the subtype of induced neurons determined their application in different types of neurodegenerative diseases. The pathological process of AD was

associated with the degeneration and loss of forebrain cholinergic neuron.³¹ The reprogrammed neurons under a set of defined conditions exhibit multiple subtypes. Abeliovich et al. derived GABAergic and glutamatergic neurons from AD patient skin fibroblasts with a combination of *Ascl1*, *Brn2*, *Myt1*, *Oligo2*, and *Zic1*.³² The reduced usage of transcription factors could purify the subtype of converted neurons. Zhang et al. combined small molecules with neurogenin 2 to efficiently convert human fibroblasts into cholinergic neurons,³³ and *Ascl1* alone induced human embryonic stem cell-reprogrammed neurons, which were mainly glutamatergic.²¹ Here, *Myt1*-induced neuron-like cells from HBVPs expressed cholinergic neuron-specific markers, including ChAT and VACHT, indicating that the converted cells were cholinergic neurons. In addition, these cells exhibited spine morphology (Figure S3), which was needed to receive excitatory inputs in neurons.³⁴ As *Myt1* was insufficient to reprogram fibroblasts to neurons,²¹ this finding thus suggests that the different

FIGURE 5 *Myt1l* overexpression induced upregulation of *Ascl1*, *Brn2*, and *Ngn2*. The relative expression of neural transcription factors *Ascl1*, *Brn2*, *Myt1l*, and *Ngn2* analyzed by real-time fluorescent quantitative PCR. *Myt1l* can activate higher *Brn2* and *Ngn2* mRNA expression levels as well as a moderate enhancement of *Ascl1* mRNA levels. Identical results were obtained from three independent experiments (n = 3)

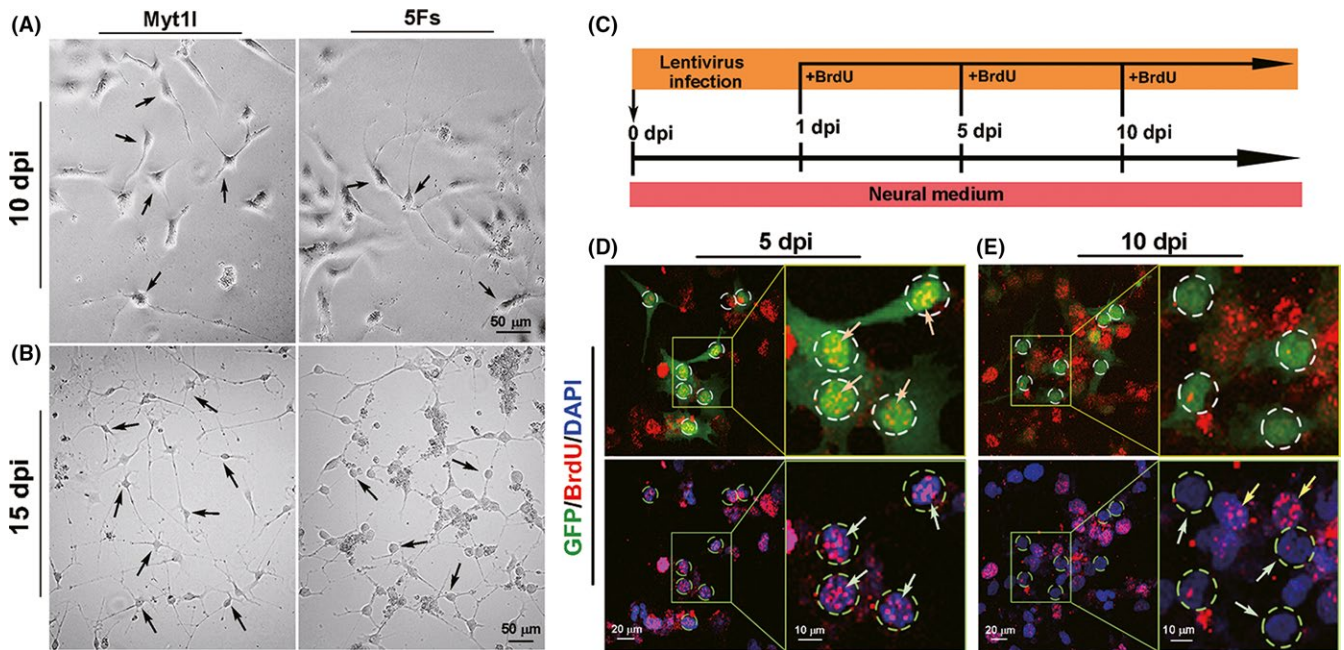
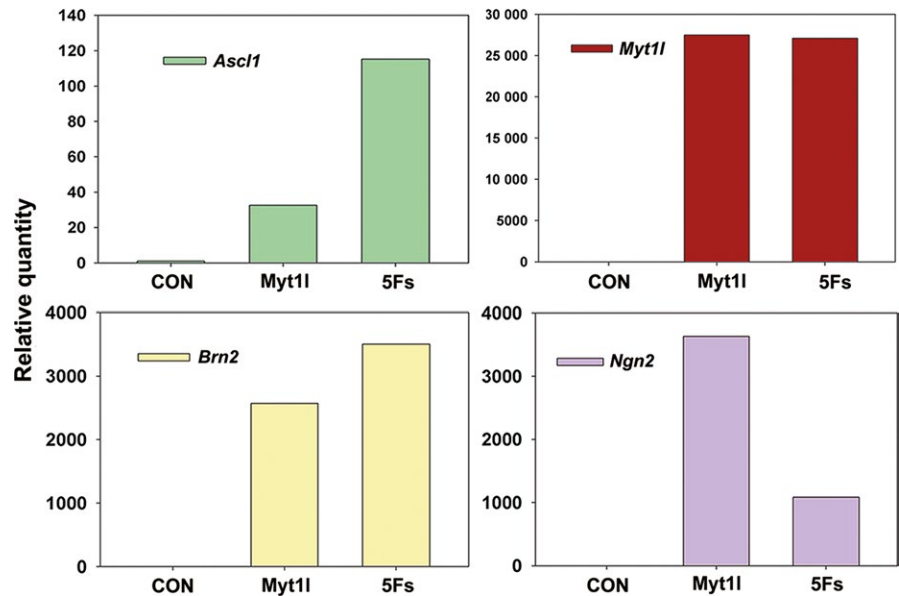


FIGURE 6 *Myt1l*/5Fs-induced neuron-like cells were directly converted from HBVPs without passing through a proliferative state. A, B, The phenotype of cell cycle exit in the progress of reprogramming. The arrows indicated the typical morphology of transitional HBVPs to neuron-like cells on day 10 (A) or day 15 (B) after infection, scale bar = 50 μ m. C, The experimental design for BrdU-labeling experiments. Cells were incubated with 10 μ mol/L BrdU for the indicated periods of time. D, HBVPs infected with 5Fs were still labeled with BrdU on day 5 after infection. GFP fluorescence indicated the infection of reprogramming factors. The arrows indicated the fluorescence of BrdU in the nuclei (blue). The right panel was the magnification pane in the left panel. E, The round square showed HBVPs infected with 5Fs were rarely labeled with BrdU after 10 dpi, indicating that neuronal conversion from HBVPs was accompanied by cell cycle exit. The arrows indicated the fluorescence of BrdU in the nuclei of non-infected cells without GFP expression. The right panel was the magnification pane in the left panel. Nuclei were stained with DAPI (blue). Scale bar = 20 μ m (left panel of figure D and E), scale bar = 10 μ m (right panel of figure D and E). Identical results were obtained from three independent experiments (n = 3)

effects of *Myt1l*-mediated HBVP reprogramming were cell-context dependent.

The tumorigenicity of cell-based therapies was a key issue that was linked to potential health risks for human research,³⁵ which

could halt the application of embryonic stem cells and induced pluripotent stem cells. The direct lineage reprogramming of somatic cells was transited in the absence of pluripotent and cell proliferation states depending on the ability of ectopic transcription factors

to force the establishment of the target cell identity gene network. This phenomenon could theoretically reduce cancer risk after transplantation. In this research, our results from the BrdU-labeling experiments indicated that neuronal conversion from HBVPs was accompanied by cell cycle exit, suggesting that *Myt1l*/5Fs-induced neuron-like cells were directly converted from HBVPs, which did not exhibit tumorigenicity and were safe for cell transplantation or in vivo reprogramming.

In conclusion, our findings provided evidence that cholinergic neurons could be produced from HBVPs by reprogramming factor-mediated fate instruction combined with the five neural conversion factors. *Myt1l* was a critical mediator of HBVP-derived neuronal reprogramming. Therefore, HBVPs not only represented a new target cell type that was suitable for direct lineage conversion to cholinergic neurons but also provided a new cell candidate for in vivo approaches. Further work is required to explore the detailed mechanisms of *Myt1l*-induced HBVPs reprogramming, and new ways of reprogramming HBVPs to neurons will be employed.

ACKNOWLEDGMENT

This work was supported in part by Projects of National Natural Science Foundation of China (81503048), Science and Technology Department of Zhejiang Province (2017C33053), Natural Science Foundation of Zhejiang Province (LY15H030007).

CONFLICT OF INTEREST

The authors declare no conflict of interest.

ORCID

Feng Han  <http://orcid.org/0000-0002-7800-9852>

REFERENCES

- Ballinger EC, Ananth M, Talmage DA, Role LW. Basal forebrain cholinergic circuits and signaling in cognition and cognitive decline. *Neuron*. 2016;91:1199-1218.
- Lu NN, Tan C, Sun NH, et al. Cholinergic Grb2-associated-binding protein 1 regulates cognitive function. *Cereb Cortex*. 2017;1-14. <https://doi.org/10.1093/cercor/bhx141>
- Moriguchi S, Han F, Nakagawasai O, Tadano T, Fukunaga K. Decreased calcium/calmodulin-dependent protein kinase II and protein kinase C activities mediate impairment of hippocampal long-term potentiation in the olfactory bulbectomized mice. *J Neurochem*. 2006;97:22-29.
- Liao MH, Xiang YC, Huang JY, et al. The disturbance of hippocampal CaMKII/PKA/PKC phosphorylation in early experimental diabetes mellitus. *CNS Neurosci Ther*. 2013;19:329-336.
- Taguchi A, Takata Y, Ihara M, et al. Cilostazol improves cognitive function in patients with mild cognitive impairment: a retrospective analysis. *Psychogeriatrics*. 2013;13:164-169.
- Wang Y, Ji X, Leak RK, Chen F, Cao G. Stem cell therapies in age-related neurodegenerative diseases and stroke. *Ageing Res Rev*. 2017;34:39-50.
- Kumar A, Narayanan K, Chaudhary RK, et al. Current perspective of stem cell therapy in neurodegenerative and metabolic diseases. *Mol Neurobiol*. 2017;54:7276-7296.
- Rosemann A. Stem cell treatments for neurodegenerative diseases: challenges from a science, business and healthcare perspective. *Neurodegener Dis Manag*. 2015;5:85-87.
- Tabar V, Studer L. Pluripotent stem cells in regenerative medicine: challenges and recent progress. *Nat Rev Genet*. 2014;15:82-92.
- Sivaraman MA, Noor SN. Human embryonic stem cell research: ethical views of Buddhist, Hindu and Catholic Leaders in Malaysia. *Sci Eng Ethics*. 2016;22:467-485.
- Hug K, Hermeren G. Do we still need human embryonic stem cells for stem cell-based therapies? Epistemic and ethical aspects. *Stem Cell Rev*. 2011;7:761-774.
- Hyun I, Lindvall O, Ahrlund-Richter L, et al. New ISSCR guidelines underscore major principles for responsible translational stem cell research. *Cell Stem Cell*. 2008;3:607-609.
- Rouaux C, Arlotta P. Direct lineage reprogramming of post-mitotic callosal neurons into corticofugal neurons in vivo. *Nat Cell Biol*. 2013;15:214-221.
- Kim J, Ambasudhan R, Ding S. Direct lineage reprogramming to neural cells. *Curr Opin Neurobiol*. 2012;22:778-784.
- Ang CE, Wernig M. Induced neuronal reprogramming. *J Comp Neurol*. 2014;522:2877-2886.
- Guarino AT, McKinnon RD. Reprogramming cells for brain repair. *Brain Sci*. 2013;3:1215-1228.
- Selvaraj V, Plane JM, Williams AJ, Deng W. Switching cell fate: the remarkable rise of induced pluripotent stem cells and lineage reprogramming technologies. *Trends Biotechnol*. 2010;28:214-223.
- Berninger B. Pericytes: a target for in vivo reprogramming? *Future Neurol*. 2013;8:365-367.
- Niu W, Zang T, Smith DK, et al. SOX2 reprograms resident astrocytes into neural progenitors in the adult brain. *Stem Cell Reports*. 2015;4:780-794.
- Karow M, Sanchez R, Schichor C, et al. Reprogramming of pericyte-derived cells of the adult human brain into induced neuronal cells. *Cell Stem Cell*. 2012;11:471-476.
- Chanda S, Ang CE, Davila J, et al. Generation of induced neuronal cells by the single reprogramming factor ASCL1. *Stem Cell Reports*. 2014;3:282-296.
- Winkler EA, Bell RD, Zlokovic BV. Central nervous system pericytes in health and disease. *Nat Neurosci*. 2011;14:1398-1405.
- Lange S, Trost A, Tempfer H, et al. Brain pericyte plasticity as a potential drug target in CNS repair. *Drug Discov Today*. 2013;18:456-463.
- Vierbuchen T, Ostermeier A, Pang ZP, Kokubu Y, Sudhof TC, Wernig M. Direct conversion of fibroblasts to functional neurons by defined factors. *Nature*. 2010;463:1035-1041.
- Ambasudhan R, Talantova M, Coleman R, et al. Direct reprogramming of adult human fibroblasts to functional neurons under defined conditions. *Cell Stem Cell*. 2011;9:113-118.
- Pang ZP, Yang N, Vierbuchen T, et al. Induction of human neuronal cells by defined transcription factors. *Nature*. 2011;476:220-223.
- Pfisterer U, Kirkeby A, Torper O, et al. Direct conversion of human fibroblasts to dopaminergic neurons. *Proc Natl Acad Sci USA*. 2011;108:10343-10348.
- Yoo AS, Sun AX, Li L, et al. MicroRNA-mediated conversion of human fibroblasts to neurons. *Nature*. 2011;476:228-231.
- Mall M, Kareta MS, Chanda S, et al. *Myt1l* safeguards neuronal identity by actively repressing many non-neuronal fates. *Nature*. 2017;544:245-249.
- Dore-Duffy P, Katychiev A, Wang X, Van Buren E. CNS microvascular pericytes exhibit multipotential stem cell activity. *J Cereb Blood Flow Metab*. 2006;26:613-624.

31. Pepeu G, Grazia Giovannini M. The fate of the brain cholinergic neurons in neurodegenerative diseases. *Brain Res.* 2017;1670:173-184.
32. Qiang L, Fujita R, Yamashita T, et al. Directed conversion of Alzheimer's disease patient skin fibroblasts into functional neurons. *Cell.* 2011;146:359-371.
33. Liu ML, Zang T, Zou Y, et al. Small molecules enable neurogenin 2 to efficiently convert human fibroblasts into cholinergic neurons. *Nat Commun.* 2013;4:2183.
34. Yuste R. Dendritic spines and distributed circuits. *Neuron.* 2011;71:772-781.
35. Lee AS, Tang C, Rao MS, Weissman IL, Wu JC. Tumorigenicity as a clinical hurdle for pluripotent stem cell therapies. *Nat Med.* 2013;19:998-1004.

SUPPORTING INFORMATION

Additional Supporting Information may be found online in the supporting information tab for this article.

How to cite this article: Liang X-G, Tan C, Wang C-K, et al. Myt1l induced direct reprogramming of pericytes into cholinergic neurons. *CNS Neurosci Ther.* 2018;24:801-809. <https://doi.org/10.1111/cns.12821>